

RESEARCH ARTICLE

First identification and characterization of ovine gammaherpesvirus type 2 in horses and artiodactyla from an outbreak of malignant catarrhal fever in Mexico

Tania Lucia Madrigal-Valencia¹ , Manuel Saavedra-Montañez¹ , Armando Pérez-Torres² , Jesús Hernández³ , Joaquim Segalés^{4,5} , Yesmín Domínguez Hernández⁶ , Irma Eugenia Candanosa-Aranda⁶ , Alfredo Pérez-Guio⁷ , Humberto Ramírez-Mendoza¹ *

1 Departamento de Microbiología e Inmunología, Facultad de Medicina Veterinaria y Zootecnia, UNAM, Mexico City, Mexico, **2** Departamento de Biología Celular y Tisular, Facultad de Medicina, Universidad Nacional Autónoma de México (UNAM), Mexico City, Mexico, **3** Laboratorio de Inmunología, Centro de Investigación en Alimentación y Desarrollo, A.C. (CIAD), Hermosillo, Sonora, Mexico, **4** Unitat Mixta d'Investigació IRTA-UAB en Sanitat Animal, Centre de Recerca en Sanitat Animal (CRESA), Campus de la Universitat Autònoma de Barcelona (UAB), Bellaterra, Barcelona, Catalonia, España, **5** Department de Sanitat i Anatomia Animals, Facultat de Veterinària, Campus de la Universitat Autònoma de Barcelona (UAB), Bellaterra, Barcelona, Catalonia, España, **6** Centro de Enseñanza, investigación y Extensión en Producción Animal en Altiplano (CEIEPAA), Facultad de Medicina Veterinaria y Zootecnia (FMVZ), Universidad Nacional Autónoma de México (UNAM), Tequisquiapan, Queretaro, Mexico, **7** División de Ciencias de la Vida, Campus Irapuato-Salamanca, Universidad de Guanajuato, ExHda El Copal, Irapuato, Guanajuato, Mexico

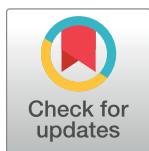
 These authors contributed equally to this work.

‡ YDH, IECA and APG also contributed equally to this work.

* betosram@comunidad.unam.mx

Abstract

Ovine gammaherpesvirus 2 (OvHV-2), a member of the genus *Macavirus*, causes sheep-associated malignant catarrhal fever (SA-MCF), a fatal lymphoproliferative disease affecting a wide variety of ungulates in addition to horses. This study described an outbreak of SA-MCF in Mexico and the identification of the OvHV-2 virus in primary rabbit testis cultures through the generation of intranuclear inclusion bodies, syncytia, immunofluorescence (IF), immunocytochemistry (ICC), immunohistochemistry (IHC), endpoint polymerase chain reaction (PCR), and partial sequencing of the *ORF75* gene. The animals involved in this outbreak showed mucogingival ulcers in the vestibule of the mouth and tongue, hypersalivation, corneal opacity, reduced food consumption, and weight loss of variable severity. These clinical signs and the histopathological findings suggested the diagnosis of SA-MCF. Buffy coat fractions from the anticoagulated blood samples of ill animals were collected and analyzed by PCR. Positive buffy coats were used to inoculate the primary cell cultures of rabbit testis to identify the virus. Small clusters of refractile cytomegalic cells, characteristic of viral cytopathic effects, were observed between 48 and 72 h post-infection. Furthermore, intranuclear acidophilic inclusion bodies (IBs) were identified in the inoculated primary culture cells, and the cytoplasm showed immunoreactivity with hyperimmune rabbit serum against OvHV-2. Moreover, in the liver histological sections from sick deer, immunoreactive



OPEN ACCESS

Citation: Madrigal-Valencia TL, Saavedra-Montañez M, Pérez-Torres A, Hernández J, Segalés J, Hernández YD, et al. (2023) First identification and characterization of ovine gammaherpesvirus type 2 in horses and artiodactyla from an outbreak of malignant catarrhal fever in Mexico. PLoS ONE 18(9): e0290309. <https://doi.org/10.1371/journal.pone.0290309>

Editor: Sherin Reda Rouby, Beni Suef University Faculty of Veterinary Medicine, EGYPT

Received: February 24, 2023

Accepted: August 6, 2023

Published: September 1, 2023

Copyright: © 2023 Madrigal-Valencia et al. This is an open access article distributed under the terms of the [Creative Commons Attribution License](https://creativecommons.org/licenses/by/4.0/), which permits unrestricted use, distribution, and reproduction in any medium, provided the original author and source are credited.

Data Availability Statement: All relevant data are within the paper and its [Supporting Information](#) files.

Funding: This study was financed by PAPIIT-UNAM (IN213321), PAPIIT-UNAM (IT201918), PAPIIT-UNAM (IT201821), and T.L. Madrigal-Valencia received a scholarship SEP-CONACYT, ID (968751).

Competing interests: The authors declare that they have no known competing financial interests or personal relationships that could have appeared to influence the work reported in this paper. We would greatly appreciate your consideration for the manuscript entitled "Isolation and identification of Ovine gammaherpesvirus type 2 in an outbreak of Malignant Catarrhal Fever in Artiodactyla and horses in Mexico" for publication as a regular manuscript at PLOS ONE. This manuscript is product of the work of Tania Lucia Madrigal-Valencia, Manuel Saavedra-Montañez, Armando Pérez-Torres, Jesús Hernández, Joaquim Segalés, Yesmín Domínguez Hernández, Irma Eugenia Candanosa-Aranda, Alfredo Pérez-Guiot, and Humberto Ramírez-Mendoza. All of us have contributed to this work and we agree on its potential publication. The manuscript has been previously reviewed by Elsevier Language Editing Services (Order reference: ASLESTD0330355). We have agreed that Dr. Humberto Ramírez-Mendoza will act as corresponding author on our behalf regarding any subsequent processing of the paper.

juxtannuclear IBs were identified with the same rabbit hyperimmune serum. The obtained sequences were aligned with the OvHV-2 sequences reported in GenBank and revealed a nucleotide identity higher than 98%. Based on the evidence provided in this study, we conclude that the outbreak of SA-MCF in the municipality of Tequisquiapan in the state of Querétaro, Mexico, was caused by OvHV-2. This is the second study reporting that horses are susceptible to OvHV-2 infection and can develop SA-MCF. We identified for the first time in Mexico, the presence of OvHV-2 in buffy coats from horses and Artiodactyla.

Introduction

Malignant catarrhal fever (MCF) is a severe lymphoproliferative disease in susceptible ungulate species of the Artiodactyla order. MCF can be caused by five viral species of the genus Macavirus: ovine herpesvirus-2 (OvHV-2), alcelaphine herpesvirus-1 (AIHV-1), alcelaphine herpesvirus 2 (AIHV-2), caprine herpesvirus 2 (CpHV-2), and an MCF virus (MCFV) in white-tailed deer (*Odocoileus virginianus*) for which domestic goats can be a carrier host [1].

The two most well-studied are OvHV-2 and AIHV-1, and their infections are asymptomatic in sheep and wildebeest reservoir populations, respectively [2]. OvHV-2 is responsible for sheep-associated malignant catarrhal fever (SA-MCF) disease in susceptible hosts, such as buffalo [3], cattle [4], deer [5], and rarely in pigs [4], and foals [6]. However, rabbits are susceptible to SA-MCF following intranasal nebulization of cell-free OvHV-2 and develop a disease similar to SA-MCF in terms of clinical signs and lesions [7, 8].

In OvHV-2, infection with non-adapted host species suggests latent infection and abortive lytic viral replication [9].

Typical SA-MCF, often referred to as the head-and-eye form, is the most common presentation of this condition in cattle [2]. Sick animals manifest pyrexia, anorexia, bilateral corneal opacity, nasal and ocular discharge, ulceration of various mucous membranes, and neurological manifestations in the terminal stages [10]. The most common gross pathological changes in SA-MCF-affected animals are erosions of the tracheal and bronchial mucosa, erythema of the turbinate mucosa, congestion, and edema of the lungs, and focal white lesions in the kidney [10]. Histopathologically, the hallmark of SA-MCF is lymphoproliferative inflammation with vasculitis involving medium-caliber arteries and veins, which is readily detected in most organs of cattle dying from acute SA-MCF [11]. Both clinical presentation and pathological features are of significant diagnostic value [12].

Detection of viral DNA by PCR in buffy coats and tissues, especially at high levels, can support the diagnosis of MCF-causing viruses (MCFV) [8]. Several serological assays have been used to detect antibodies against SA-MCF, but all assays use Alcelaphine herpesviruses as antigens, predominantly AIHV-1 because these viruses can be propagated in vitro [13]. These assays include virus serum neutralization (VN), immunoblotting (IFA), enzyme-linked immunosorbent assay (ELISA), competitive inhibition ELISA (cELISA), immunofluorescence assay (IF), immunoperoxidase assay (IPT), and drug complement fixation test [14–20]. However, the VN has very limited use in the detection of antibodies in animals infected with OvHV-2, and polyclonal antibody-based assays (ELISA, IFA, and IPT, among others) can detect antibodies against multiple epitopes of AIHV-1 [21, 22]. To increase specificity, an ELISA has been developed using an Ov8 recombinant protein from OvHV-2 [23].

For the in vitro isolation of MCFV, primary cultures of bovine thyroid (BTh), bovine kidney (BK), bovine embryonic kidney (BEK), and calf testis (CT) cells have been used [22, 24,

25]. On the other hand, Hristov et al. (2016) described the use of primary rabbit kidney (RK) cell cultures and permanent cell cultures (Madin Darby bovine kidney (MDBK) cell line, embryonic bovine tracheal (EBTR) cell line, green monkey kidney cell line (VERO), and monkey cell line (MA-104)) for the isolation of the OvHV-2 virus. However, they mention that additional investigations are needed to confirm which type of OvHV-2 or AlHV-1 viral isolation they performed [26].

Cases of SA-MCF have been documented in North America, and economic losses to bison producers have been estimated at approximately US\$1 million [27]. However, the direct economic losses associated with SA-MCF morbidity and mortality in Brazil were estimated at US \$215,592 and US\$214,368, respectively. If the data were projected nationally, it would result in a projected economic loss of US\$3.5 to US\$4.8 billion for the cattle industry in Brazil [28].

The first case of SA-MCF in Mexico was documented in Mexico City in a 6-year-old Holstein cow in 1969, which presented head and ocular clinical manifestations in addition to perivascular lymphoid infiltrate in various organs. However, the diagnosis was based only on a clinicopathological study [29]. More recently, an outbreak of SA-MCF occurred in the municipality of Tequisquiapan in the state of Queretaro, Mexico, affecting many animals that developed a typical head-and-eye clinical presentation.

Only one study has been carried out thus far investigating OvHV-2 in Mexico, as it is considered an exotic disease. Moreover, the economic and epidemiological impact of SA-MCF and the distribution and molecular characterization of the OvHV-2 virus in this country are unknown. Therefore, this study aimed to identify and characterize the OvHV-2 virus that causes the SA-MCF outbreak in horses and *Artiodactyla* kept at the Centro de Enseñanza, Investigación y Extensión en Producción Animal en Altiplano (CEIEPAA), Tequisquiapan, Queretaro, Mexico.

Material and methods

Ethics statements

All experimental procedures involving animals were conducted following the Institutional Subcommittee for the Care and Use of Experimental Animals of the Universidad Nacional Autónoma de México (UNAM) (SICUAE.DC-2020/3-5).

Sampling location

Sampling was performed at the CEIEPAA, belonging to the UNAM, located in Tequisquiapan, state of Queretaro, Mexico. This farm has an area of 186 ha. It is based on a semi-intensive production system with multiple species: deer (European red), dairy cows (Holstein, Jersey, and crosses), feedlot cattle (Limousin), sheep (Suffolk, Katahdin, and crosses), goats (Alpine Frances, Saanen, Toggenburg, and Boer) and horses (English thoroughbred, quarter horse, appendix, Portuguese, Santa Gertrudis, and Creole) (Fig 1). The species were separated between 1.14 and 2.8 km [30].

The outbreak chronology

From August to December 2018, a vesicular disease occurred that affected all species of animals belonging to the CEIEPAA farm, and the United States-Mexico Commission for the Prevention of Foot-and-Mouth Disease and other Exotic Animal Diseases (CPA) took samples of serum, blood, epithelium of ulcerative lesions of the oral mucosa, deer organs (tongue, brain, submandibular lymph nodes, kidney, and spleen), and nasal swabs to carry out differential



Fig 1. The geographical location of Tequisquiapan, Queretaro (Mexico), where the CEIEPAA is located (Modified from INEGI, 2023; <https://www.inegi.org.mx/app/areasgeograficas/?ag=07000022#collapse-Mapas>).

<https://doi.org/10.1371/journal.pone.0290309.g001>

diagnoses of vesicular diseases [30]. In January 2019, UNAM conducted targeted sampling to identify and characterize the OvHV-2 virus.

Supplementary tests

The serum samples were analyzed with ELISA tests to diagnose foot-and-mouth disease virus (FMDV) and vesicular stomatitis virus (VSV). On the other hand, samples of epithelium, blood, deer organs (tongue, brain, submandibular lymph nodes, kidney, and spleen), and nasal swabs were used to perform different molecular diagnoses: PCR or reverse transcription polymerase chain reaction (RT-PCR) for FMDV, infectious bovine rhinotracheitis virus (IBRV), Indiana and New Jersey VSV, parapoxvirus (PRV), bluetongue virus (BTV), and contagious ecthyma virus (CEV). In addition to viral isolation of VSV (Table 1).

Post-mortem evaluation

Of the 14 deer that died during the 2018 SA-MCF outbreak, 9 deer were assessed post-mortem because 5 were in an advanced state of decomposition. The results of the post-mortem evaluation were published by Pérez et al. (2022) [30]. Our current research presents the results of two of these deer (#172 and #174), which were chosen due to the severity of their clinical signs and lesions. Cornea, lymph nodes, tongue, rumen, liver, lung, and kidney samples were taken and fixed by immersion in 10% buffered formalin solution and routinely processed for paraffin embedding and sectioning using hematoxylin and eosin (H&E) staining for observation and histopathological analysis.

Clinical sample collection and preparation

In January 2019, a new sampling was performed. Nevertheless, this time was aimed at animals that the CPA had previously tested positive for OvHV-2 by PCR, including those that still had ulcerative lesions (11 horses) and some healthy animals. The purpose of this sampling was to identify and characterize the OvHV-2 virus. Approximately 30 blood samples from each animal species were obtained in Vacutainer® tubes. Subsequently, the buffy coats were separated according to the methodology described by English & Andersen (1974) [31], and after they were stored at -196°C until processing for viral identification and PCR.

Table 1. Affected species, testing by PCR of other viruses and percentage of positive animals for OvHV-2.

Affected species	*Previous Diagnoses/ Results (PCR)	**Clinical signs	Total, population/sick/ dead	***Total number of animals sampled by CPA, OvHV-2 PCR positive, and percentage of positive	****Sampled animals, OvHV-2 PCR-positive and percentage of positive
Horses	VSV/ (-)	MUMV, UT, LFC, WL	39/14/0	35 [2] (5.71%)	39 [9] (23%)
Feedlot cattle	IBRV, VSV, PRV, FMDV, BTV/ (-)	MUMV, HS, LFC, WL	109/8/0	38 [8] (21.05%)	30 [11] (36%)
Dairy cattle	IBRV, VSV, PRV, FMDV, BTV/ (-)	MUMV, HS, LFC, WL	169/15/0	51 [6] (11.76%)	32 [5] (15%)
Resident goats	IBRV, VSV, PRV, FMDV, BTV/ (-)	-	271/0/0	30 [7] (23.33%)	32 [19] (59%)
Goats in the quarantine area	IBRV, VSV, PRV, FMDV, BTV, CEV/ (-)	MUMV	97/7/0	98 [35] (35.71%)	32 [8] (25%)
Sheep	IBRV, VSV, PRV, FMDV, BTV, CEV/ (-)	MUMV	246/37/0	67 [22] (32.83%)	30 [26] (86%)
Deer	IBRV, VSV, PRV, FMDV, BTV, CEV/ (-)	MUMV, HS, CO, LFC, WL	103/21/14	17 [8] (47.05%)	18 [8] (44%)
Total			1034/65/14	336[88](26.19%)	213[86] (40.3%)

Results of the nested end-point PCR for detecting the OvHV-2 virus in buffy coat samples of different species.

[] = positive to PCR, () = percentage of animals positive to PCR.

*Infectious bovine rhinotracheitis virus (IBRV), vesicular stomatitis virus serotypes Indiana and New Jersey (VSV), parapoxvirus (PRV), foot and mouth disease virus (FMDV), bluetongue virus (BTV), contagious ecthyma virus (CEV).

**mucogingival ulcers in the mouth vestibule (MUMV), ulcers in the tongue (UT), hypersalivation (HS), corneal opacity (CO), lower food consumption (LFC), and weight loss (WL).

*** Total number of animals sampled by CPA from August to December 2018

**** Total number of animals sampled by UNAM during January 2019

<https://doi.org/10.1371/journal.pone.0290309.t001>

Nested endpoint polymerase chain reaction (PCR) for OvHV-2 detection

Nested endpoint PCR was specific for the *ORF75* segment of OvHV-2, which encodes phosphoribosyl-formyl-glycinamide synthase (FGARAT), which participates in purine metabolism and the production of viral tegument proteins [32].

Genetic material was extracted according to the manufacturer's instructions for the High Pure PCR kit (Roche, Basel, Switzerland) [33]. Primer pairs designed by Baxter et al. (1993) were used, and nested PCR was performed according to the method described by Li et al. (1995), with some modifications [21, 32]. Briefly, in the first and second amplification reactions, 10 μ M of each primer set was used, and the reaction volume was adjusted to 25 μ L. A PCR Master Mix 5X (Taq-Load) was used. All reactions were performed using a GeneAmp® PCR System 9700 (Applied Biosystems, Waltham, MA, USA). A positive result generated a 238-bp band in the second amplification.

A bovine blood sample that tested positive for OvHV-2 by PCR and partial sequencing (ref. 6191), donated by CPA, was used as a positive control, and nuclease-free water was used as the negative control.

Primary cell cultures

The primary cell culture was prepared using testes from 2-month-old male rabbits, which were humanely euthanized (SICUAE.DC-2020/3-5)]. Testes were washed five times with Hanks

balanced salt solution (HBSS, Gibco, Life Technologies) supplemented with penicillin (100 U/mL, Gibco, Life Technologies), streptomycin (100 g/mL, Gibco, Life Technologies) and fungizone (2.5 g/mL, Gibco, Life Technologies). They were then placed in a sterile Petri dish where each testis's tunica albuginea and connective tissue septa were dissected with sterile scissors. With the help of sterile forceps, manual cuts were made to obtain fragments smaller than 0.5 cm² from both testes. The testes fragments were trypsinized for 1 h at 37°C under constant agitation using 0.25% trypsin-EDTA with phenol red (Gibco, Cat: 25200056) at a 1:5 ratio.

After incubation, the detached cells were filtered through a funnel with sterile gauze, and the filtrate was collected in a centrifuge tube and centrifuged at 800 × g for 10 min. The supernatant was discarded, and the pellet of cells was resuspended in Dulbecco's modified Eagle's medium (DMEM) supplemented with 10% fetal calf serum. Approximately 0.5 × 10⁶ cells/mL were seeded per bottle. Cultures were maintained in 25 cm² flasks (Nunc, Roskilde, Denmark) at 37°C with a 5% CO₂ atmosphere. Cells were monitored daily under an inverted Olympus microscope (IX71) with a 10× objective (Olympus Corporation, Shinjuku City, Tokyo, Japan), and after 2 days, the DMEM supplemented with 10% fetal bovine serum was changed to a similar fresh medium.

Inoculation of primary cell cultures

For the identification of OvHV-2, 25-cm² bottles with 80% cell confluence were used. Each bottle was inoculated with 200 μL of buffy coat lysate (PCR positive for OvHV-2). Lysates were obtained by freezing and thawing the buffy coats from each of the six species naturally infected with OvHV-2 (deer, dairy cattle, feedlot cattle, sheep, goats, and horses). Inoculated cells were propagated in DMEM supplemented with 5% fetal calf serum and incubated at 37°C with a 5% CO₂ atmosphere. The flasks with the inoculated cells were observed every 24 h for 7 days using an Olympus inverted microscope (IX71) with a 10× objective (Olympus Corporation) to identify the specific cytopathic effect of OvHV-2 [26].

At least four blind passages were performed in all species except horses, in which fourteen blind passages were needed for virus adaptation to cell culture and cell-free virus production. Bottles with inoculated cells were frozen and thawed when cytopathic changes were observed in the monolayers (refractile cytomegalic cell foci, syncytia, or 50% destruction of the monolayer). Then, the culture supernatant was centrifuged at 1200 × g for 10 min, and the final supernatant was divided into small aliquots and stored at -80°C until use. For consecutive passages, fresh monolayers were prepared and inoculated with the virus supernatant mentioned above. When cytopathic changes were observed in the monolayers, the bottles with the inoculated cells were processed as mentioned above. Following the cytopathic changes of the monolayers, culture supernatants from the four blind passages were identified for the ORF75 segment of the OvHV-2 virus DNA by nested PCR. As a negative control, a 25-cm² bottle with 80% cell confluence was inoculated with 200 μL of buffy coat lysate from OvHV-2-negative horses.

The virus titer was quantified from the cell-free supernatants of the 4th blind passage of all the species and from the 3rd to the 14th blind passages of the horse. Flat-bottomed 96-well plates were used as described by Reed and Muench [34]. To analyze the plates under a microscope, they were fixed 72 h post-infection with 4% paraformaldehyde diluted with distilled water and stained with 0.5% crystal violet diluted in 96° alcohol.

To observe intranuclear inclusion bodies (IBs), a 24-well plate at 80% cell confluence was inoculated with 200 μL of each of the four blind passages described above. The inoculated cells were propagated with DMEM supplemented with 2% fetal calf serum and incubated at 37°C for 24 h in a 5% CO₂ atmosphere. Subsequently, the supernatant was removed, and the cells

were fixed with 4% paraformaldehyde. Finally, hematoxylin stain was added for 1 min, washed with distilled water, and stained with eosin stain for 30 s. The bottom of each well was covered with glycerol and a coverslip. The intranuclear IBs were observed under an Olympus inverted microscope (IX71) with a 10× objective (Olympus Corporation). As a negative control, a 4-well plate was left at 80% cell confluence and inoculated with 200 μ L of the buffy coat lysate from OvHV-2-negative horses; otherwise, the remaining analytical procedure was identical to that given above.

Viral replication kinetics

The kinetics of viral replication were analyzed from the cell-free supernatants of the 4th, 5th, and 14th passages of the buffy coat lysate from horses. Primary cultures of rabbit testis grown in 96-well flat bottom plates were inoculated and processed according to the technique of Reed and Muench [34]. Briefly, primary cultures were inoculated with serial 10-fold dilutions of each of the samples in quadruplicate per dilution. The inoculum was then removed at different time points (24, 48, 72, 96, and 120 h post-infection), and the plates were fixed with 4% paraformaldehyde for 10 min and stained with 0.5% crystal violet. Graphics were prepared using GraphPad Prism 9.5.1 software (GraphPad, USA).

Partial sequencing of the ORF75 gene

Partial sequencing of the *ORF75* gene was performed from the fourth blind passage obtained by inoculating primary cultures with buffy coat lysate from different animal species (deer, dairy cattle, feedlot cattle, sheep, goats, and horses). Furthermore, partial sequencing of the CPA-donated positive control was performed. The seven samples were amplified by endpoint PCR to obtain a 422-bp fragment corresponding to a segment of the *ORF75* gene, and 300 ng of each PCR product was sequenced by bidirectional capillary electrophoresis through Sanger sequencing using external PCR primers as sequencing primers (MCF 556 and MCF 755) [32]. Electropherograms from each pair of sequencing reactions were edited and assembled with the Biological Sequence Alignment Editor (BioEdit), v 7.2.0; [35]. Sequences were aligned using MEGA 11 software [36].

Phylogenetic analysis

The seven consensus sequences obtained using BioEdit software were compared with partial sequences of the *ORF75* gene reported in GenBank [35]. For the phylogenetic analysis, the alleles of high and low similarity for *ORF75* were selected using the BLAST (Basic Local Alignment Search Tool) of the NCBI (National Center for Biotechnology) [37].

Finally, the seven sequences were phylogenetically analyzed with sequences from the genus Macavirus (OvHV-2, AIHV-1, and AIHV-2) and human gammaherpesvirus types 4 and 8 (HHV-4 and HHV-8). The substitution model was selected with Jmodeltest, indicating that the Tamura-Nei model was the most appropriate for this data set [38, 39]. The analysis was performed with MEGA 11 software using the maximum likelihood method with 1,000 replicas [36].

The seven consensus nucleotide sequences of the *ORF75* gene fragment amplified in this work have been submitted to the GenBank public database and have been assigned the following accession numbers: ON375578 (horses), ON375579 (goats), ON375580 (deer), ON375581 (dairy cattle), ON375582 (feedlot cattle), ON375583 (sheep) and ON375584 (CPA positive control).

Hyperimmune serum

To prepare an anti-OvHV-2 hyperimmune serum, we followed a protocol from a previous study by Orós et al. (1997), with some modifications. Three 9-week-old New Zealand white rabbits weighing approximately 1.7 kg and negative for OvHV-2 by nested endpoint PCR were used [40].

Rabbits were inoculated intramuscularly with the cell-free supernatant from the fourth blind passage of the horses (Tissue Culture Infectious Dose $10^{4.19}$ TCID₅₀/mL) dissolved in phosphate-buffered saline (PBS) and a 2% Alhydrogel® (w/v) aqueous suspension of aluminum hydroxide gel adjuvant (InvivoGen). The supernatant from the previously mentioned fourth blind passage was inactivated with 0.2% formaldehyde diluted in distilled water.

Rabbits were housed in stainless-steel cages with wire mesh, fed commercial pellets, and had free access to running water. The animals were kept at a temperature of 23–25°C. After an acclimatization period, the rabbits received weekly intramuscular inoculation for 5 weeks. Subsequently, the rabbits were tranquilized (acepromazine 1 mg/kg), and their hearts were bled and then euthanized with an overdose of pentobarbital. The serum obtained was stored at -20°C until its subsequent use in immunofluorescence (IF), immunocytochemistry (ICC), and immunohistochemistry (IHC) techniques.

Immunocytochemistry (ICC) and immunofluorescence (IF) techniques

To perform the ICC and indirect IF analyses, we modified the methodology described by Rositer (1981). Two 24-well plates were used with a cell confluence of 80%, and the wells were inoculated with 200 µL of each of the four blind passages obtained previously [14].

Subsequently, they were incubated at 37°C for 72 h and fixed with 4% paraformaldehyde diluted in distilled water for 10 min at room temperature. The cells were permeabilized with 0.2% Triton X-100 for 5 min at room temperature. The plates were then washed three times with PBS. For ICC, endogenous peroxidase was inhibited by incubation with 3% hydrogen peroxide diluted in distilled water for 15 min and washed three times with distilled water. To reduce background noise, the two plates were incubated with 2.5% bovine serum albumin diluted in Tris-HCl buffer for 30 min at 37°C. Next, the two plates were incubated with anti-OvHV-2 rabbit hyperimmune serum diluted 1:5 in 0.1% albumin for 24 h at 4°C. After three washes with PBS, peroxidase-conjugated protein A was added to the ICC plate diluted 1:16 in 0.1% albumin and incubated for 1 h at 37°C, followed by three washes with PBS. The chromogen (hydrogen peroxide and 3,3'-diaminobenzidine) was added for 5 min, and the reaction was stopped with distilled water. Cells with positive immunoreactivity to the anti-OvHV-2 hyperimmune serum presented an insoluble brown coloration. The plate used for IF was processed in the same way as for ICC; however, endogenous peroxidase inhibition was omitted, and a fluorescein isothiocyanate (FITC)-conjugated anti-rabbit conjugate (anti-rabbit IgG) diluted 1:20 in 0.1% albumin was used as the conjugate. Cells with positive immunoreactivity to the anti-OvHV-2 hyperimmune serum were determined as those that presented an apple-green fluorescent emission at 520 nm. Immunoreactivity of the plates was observed using an Olympus epifluorescence inverted microscope (IX71) (Olympus Corporation). Uninoculated primary cell cultures and sera from rabbits negative for SA-MCF were used as negative controls.

Immunohistochemistry

The specificity of the anti-OvHV-2 hyperimmune serum was evaluated in the liver of deer that died naturally during the SA-MCF outbreak at the CEIEPAA farm. This technique was performed as described by Headley et al. (2022), with some modifications [41]. Liver sections

were mounted on positively charged slides (BiocareTM), deparaffinized with xylene, rehydrated with 0.1 M Tris-HCl buffer (pH 7.2), and transferred to a glass Coplin staining bottle with citrate buffer (0.1 M [pH 6.0]) for antigen retrieval. The procedure was performed in a pressure cooker for 10 min at 200°C. The slides were then left for 15 min at room temperature (RT) in a Coplin jar containing 0.1 M Tris-HCl buffer (pH 7.2). Subsequently, endogenous peroxidase was inhibited using 3% hydrogen peroxide diluted in distilled water. To reduce non-specific background staining, slides were incubated for 1 h at 37°C in a solution containing 0.1 M Tris-HCl buffer (pH 7.2), 1% dry milk, and 0.01% Triton X-100. This solution was decanted, and the slides were incubated overnight at 4°C with rabbit anti-OvHV-2 hyperimmune serum diluted 1:5 in 0.1 M Tris-HCl buffer (pH 7.2) with bovine serum albumin (BSA) at 0.1%. After three washes with 0.1 M Tris-HCl buffer (pH 7.2), the slides were incubated with a peroxidase-coupled anti-rabbit IgG diluted 1:50 in 0.1 M Tris-HCl buffer (pH 7.2) with 0.1% BSA for 1 hour at RT. After three washes with 0.1 M Tris-HCl buffer (pH 7.2), a mixture of 3% hydrogen peroxide and 3,3'-diaminobenzidine was added to the slides to reveal the binding of anti-OvHV-2 hyperimmune serum in deer hepatocytes. Finally, the slides were counterstained with hematoxylin for 1 min. Positive immunoreactivity to anti-OvHV-2 hyperimmune serum was observed as an insoluble brown stain in the cytoplasm of the hepatocytes. A deer liver sample slide was used and processed as described above as a negative control, but anti-OvHV-2 rabbit hyperimmune serum was omitted.

Results

The outbreak chronology

On August 29, 2018, the first case of SA-MCF was suspected during the necropsy of a six-month-old goat belonging to the quarantine area that had recently been donated to the farm. The animal showed ulcerative lesions on the tongue and larynx; in addition, vasculitis and perivasculitis in different tissues were observed histopathologically. In September, 6 goats from the quarantine area and 15 Holstein cows had ulcerative lesions on the oral mucosa. SA-MCF is considered an exotic disease with mandatory reporting in Mexico, so on September 2, 2018, the outbreak was reported to the CPA. On September 3, the CPA first sampled the animals with and without clinical signs of all animal species to confirm the diagnosis. One week later, the CPA released the results, and the goats and dairy cows were confirmed to be negative for FMDV and VSV by ELISA and PCR. However, on October 4, 2018, six of the Holstein cows were PCR positive for OvHV-2 and negative for IBRV, PRV, and BTV.

By November, the disease had already spread to deer, feedlot cattle, and sheep. At that time, 21 deer had ulcerative lesions in the oral mucosa, and 5 blood samples and 3 tissues of these animals were PCR positive for OvHV-2 and negative for IBRV, VSV, PRV, FMDV, and CEV. On the other hand, 8 Limousine cattle had ulcerative lesions and were also positive for OvHV-2 by PCR. Finally, 10 sheep showed lesions suggestive of MCF, and on November 21, 2018, they were confirmed as positive for OvHV-2 by PCR.

In December 2018, 27 sheep had slight ulcerative oral cavity lesions and at the end of this month, the virus spread to horses; 14 of them displayed ulcerative lesions on the lips although only 2 were PCR positive for OvHV-2 and negative for VSV by RT-PCR and viral isolation (Table 1). Most of the species recovered in a period of 20 days. However, the disease extended in deer for a few more days due to the severity of the ulcerative lesions in the oral mucosa, which made it impossible for them to eat.

During the outbreak, all animals of the farm received medical treatment based on immunological stimulants, vitamins A, D, and E, and the drinking water was alkalized. In November 2019 and 2020, there were two new outbreaks. Affected animals showed clinical signs similar

to those observed in 2018. However, in these two new outbreaks, the most affected species was the horse due to the severity of the ulcers. In addition, in 2020, parturient goats also had ulcerative lesions on the oral mucosa.

Post-mortem evaluation

The animals affected during the outbreak at CEIEPAA showed mucogingival ulcers in the buccal vestibule and tongue, hypersalivation, lower food consumption, weight loss, and corneal opacity (Fig 2). The two deer (#172 and #174) had marked retromandibular lymphadenomegaly, congested and edematous tongue, with ulcers on its dorsal part and the base. In addition, focal ulcers were observed in the rumen pillars, covered by a fibrinous pseudomembrane. The liver was slightly enlarged and congested. The main microscopic lesions observed were vasculitis and perivasculitis with fibrinous necrosis of blood vessels in the tongue and rumen, epithelial erosion, edema, and neovascularization of the cornea. The retromandibular lymph nodes showed lymphoid hyperplasia. The liver showed multifocal hepatic necrosis and cytoplasmic eosinophilic IB (Fig 3). No post-mortem lesions were observed in the kidney or lung.

Buffy coat samples

A total of 213 buffy coat samples from the animals with clinical signs compatible with SA-MCF were tested by nested end-point PCR; 86 were positive (40.38%), and 127 were

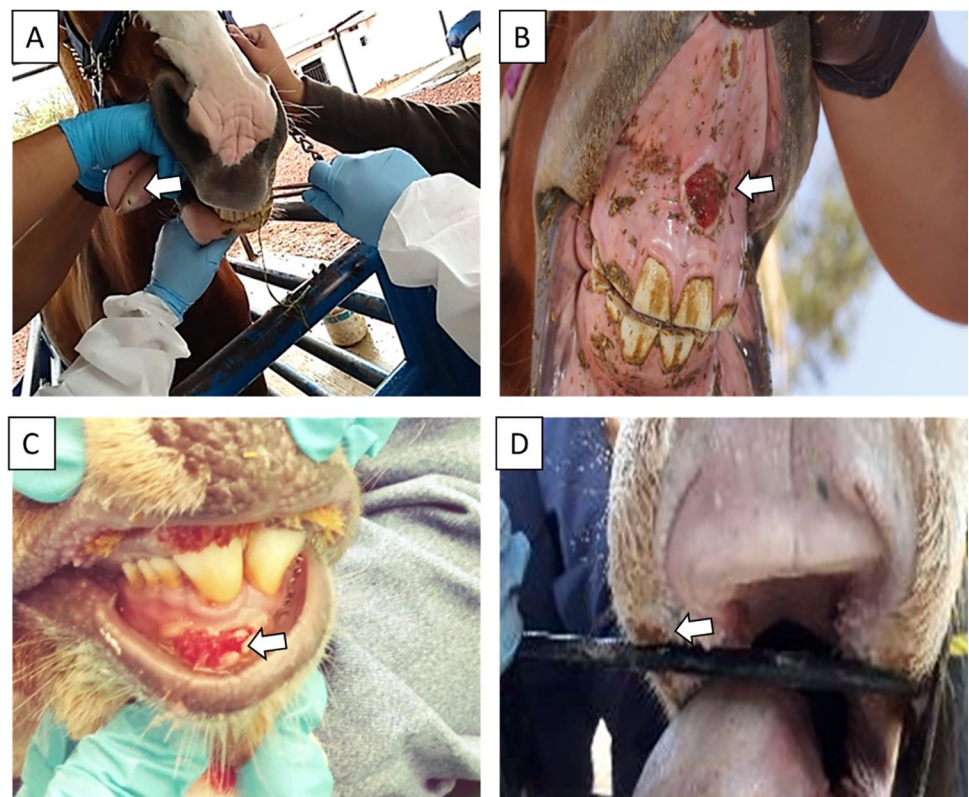


Fig 2. Ulcerative lesions in the oral mucosa of animals that survived the 2018 SA-MCF outbreak and deer that died 5 days after disease onset in CEIEPAA, Tequisquiapan, Queretaro, Mexico. (A) Horse with an ulcer on the apex of the tongue, (B) horse with an ulcer on the mucosa of the gums, (C) deer with ulcers on the mucosa of the upper and lower gums, (D) dairy cattle with an ulcer on the corner of the mouth. White arrows point to ulcers.

<https://doi.org/10.1371/journal.pone.0290309.g002>

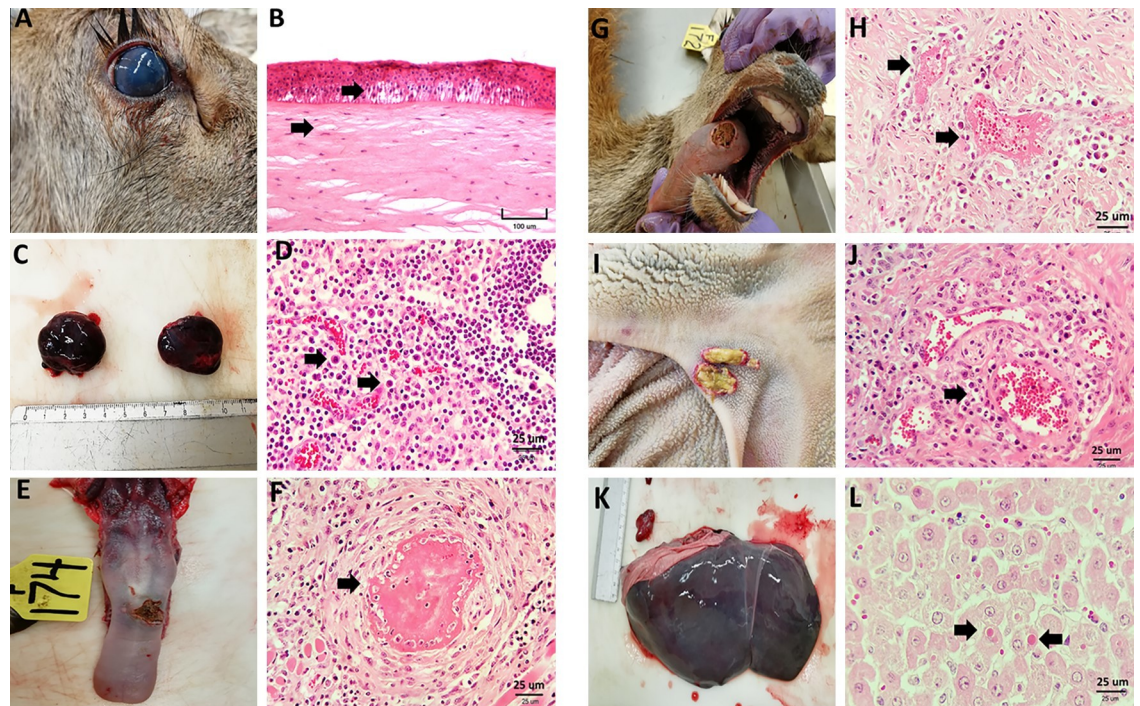


Fig 3. Post-mortem lesions were observed in deer #172 and #174 that died during the 2018 SA-MCF outbreak in CEIEPAA, Tequisquiapan, Queretaro, Mexico. (A) Corneal opacity, (B) cornea with edema and detachment of the corneal epithelium (black arrows), (C) enlarged, congested, and edematous retromandibular lymph nodes, (D) parafollicular region with numerous lymphocytes, plasma cells, and lymphoblasts (black arrows), (E) tongue with loss of epithelium continuity (ulcer) in the dorsal portion, (F) tongue with vasculitis and fibrin thrombus that occludes the lumen and fibrinoid necrosis (black arrow), (G) tongue with an ulcer in the dorsal portion of the tongue, with food encrustation, (H) tongue with thrombosis and infiltrate lymphoplasmacytic and lymphoblastic perivascular inflammation (black arrows), (I) rumen with focal ulcers in the pillar covered by a pseudomembrane, (J) rumen with perivascular inflammation composed of lymphocytes, plasma cells and lymphoblasts (black arrow), (K) enlarged and congested liver (hepatomegaly), (L) liver with areas of necrosis and cytoplasmic eosinophilic IB (black arrows).

<https://doi.org/10.1371/journal.pone.0290309.g003>

negative (59.62%). The PCR results revealed that resident goats and sheep had the highest percentage of animals positive for OvHV-2, whereas dairy cattle and horses had the lowest number of positive animals (Table 1).

Inoculation of primary cell cultures

The cytopathic effect (CPE) caused by the buffy coat lysate pools, characterized by changes in primary culture morphology, generated small clusters of refractile cytomegalic cells between 48 and 72 h post-infection and was similarly induced with the six buffy coat lysate pools used (Fig 4).

Buffy coat lysates from sheep and goats induced marked CPE with 50% destruction of the monolayer from the first passage to 72 h and 100% between 96 and 120 h post-infection. Similarly, the percentage of CPE increased from the second passage and fourth passage onward for goat and sheep buffy coat lysates, respectively (Table 2). In contrast, primary cell cultures inoculated with buffy coat lysate pools from horses, dairy cattle, feedlot cattle, and deer showed low CPE, ranging between 20 and 30% in the first and second passages, respectively. In contrast, in the third and fourth passages, monolayer destruction increased to 50% and 90% at 72 h post-infection (Table 2).

In cell cultures, viral titers obtained from the cell-free supernatants of the 4th blind passage at 72 h post-infection were as follows: horses $10^{4.19}$ TCID₅₀/mL, goats $10^{3.8}$ TCID₅₀/mL, deer

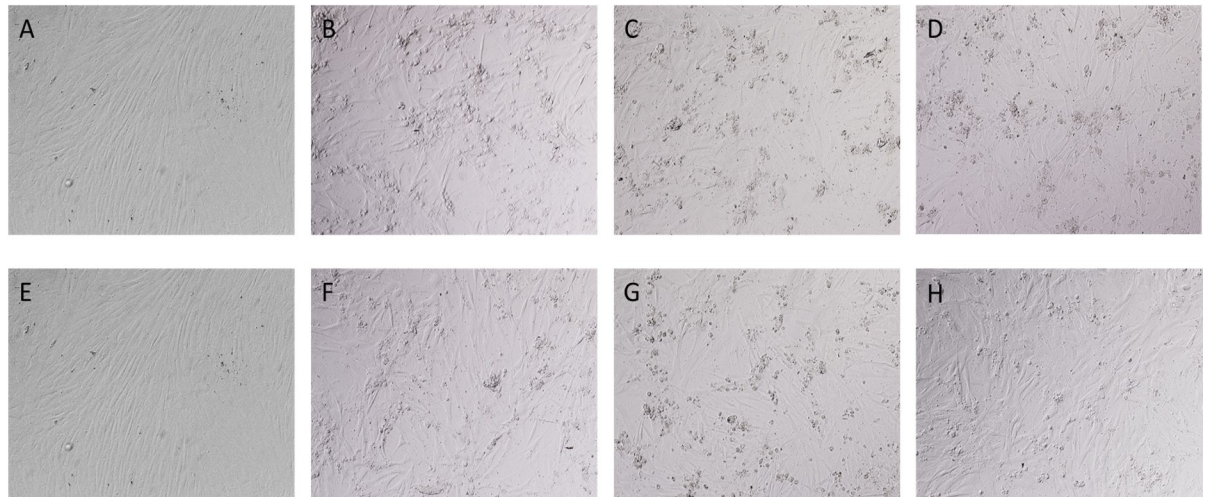


Fig 4. Cytopathic effect in primary cell cultures of rabbit testis cells inoculated with buffy coats of the different animal species affected during the SA-MCF outbreak at 72 h post-infection. (A) Negative controls, (B) fourth blind passage from horses, (C) fourth blind passage from sheep, (D) fourth blind passage from sheep, (E) negative control, (F) fourth blind passage from deer, (G) fourth blind passage from dairy cattle, (H) fourth blind passage from feedlot cattle. Magnification: 100X.

<https://doi.org/10.1371/journal.pone.0290309.g004>

$10^{3.3}$ TCID₅₀/mL, dairy cattle $10^{3.5}$ TCID₅₀/mL, feedlot cattle $10^{2.8}$ TCID₅₀/mL and sheep $10^{3.5}$ TCID₅₀/mL.

Viral titers of the cell-free supernatants of the 3rd to 14th passages from the buffy coat lysate from horses were collected at 72 h post-infection in each passage, and the CPE in crystal violet-stained wells was read (Fig 5). We determined that the viral titer of the 3rd passage was $10^{3.3}$ TCID₅₀/mL, while the viral titers of passages 4, 5, 6, 7, 8, 9, 10, and 11 ranged from 10^4 TCID₅₀/mL to $10^{4.96}$ TCID₅₀/mL, which were very similar. However, an increase in titers was observed in passage 12, 13, and 14 viruses with titers of $10^{5.52}$ TCID₅₀/mL, $10^{6.46}$ TCID₅₀/mL, and $10^{6.67}$ TCID₅₀/mL, respectively.

Intranuclear acidophilic IBs were observed in primary cell cultures of rabbit testis cells inoculated with the cell-free supernatants of the four blind passages at 24 h post-infection. However, in the wells containing the cells inoculated with cell-free supernatants of the fourth blind passages from goats and horses, more than five IBs were observed (Fig 6). In contrast, in wells inoculated with cell-free supernatants of the fourth blind passages from dairy cattle, feedlot cattle, sheep, and deer, fewer than three IBs were observed in the entire well.

Table 2. Cytopathic effect in primary cell cultures.

Affected species	CPE*	CPE*	CPE*	CPE*
	1° passage	2° passage	3° passage	4° passage
Horses	20–30%	20–30%	50%	90–100%
Feedlot cattle	20–30%	20–30%	20–30%	90–100%
Dairy cattle	20–30%	20–30%	90–100%	90–100%
Goats	50%	90–100%	90–100%	90–100%
Sheep	50%	20–30%	20–30%	90–100%
Deer	20–30%	20–30%	50%	90–100%

Percentage of cytopathic effect in primary cell cultures of rabbit testis.

CPE* = Cytopathic effect (percentages reflect the degree of cellular monolayer destruction)

<https://doi.org/10.1371/journal.pone.0290309.t002>

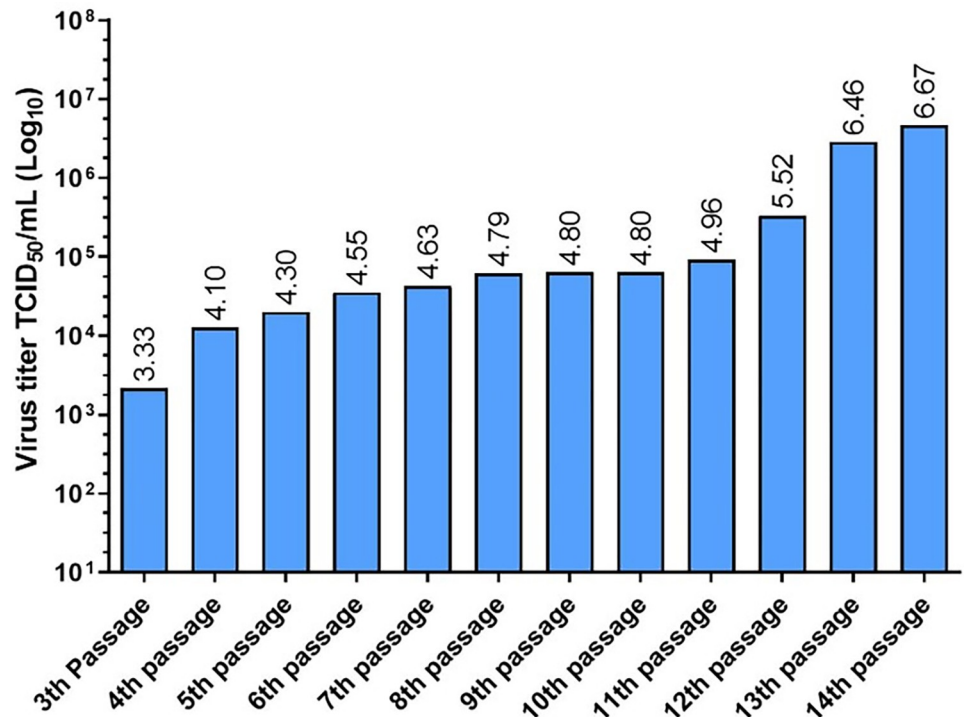


Fig 5. Virus titration of the supernatants from the 3rd to 14th passages of the buffy coat lysate from horses. Continuous passage of the buffy coat lysate from horses in primary rabbit testis cultures led to an increase in viral titer.

<https://doi.org/10.1371/journal.pone.0290309.g005>

Nested end-point PCR for OvHV-2 detection

DNA was extracted from the cell-free supernatants of the four blind passages obtained from the infection of the primary cultures with buffy coat lysate pools from the different animal species affected during the SA-MCF outbreak. The cell-free supernatants from horses, goats, and dairy cattle were positive by PCR for OvHV-2 from the first passage. The cell-free supernatants

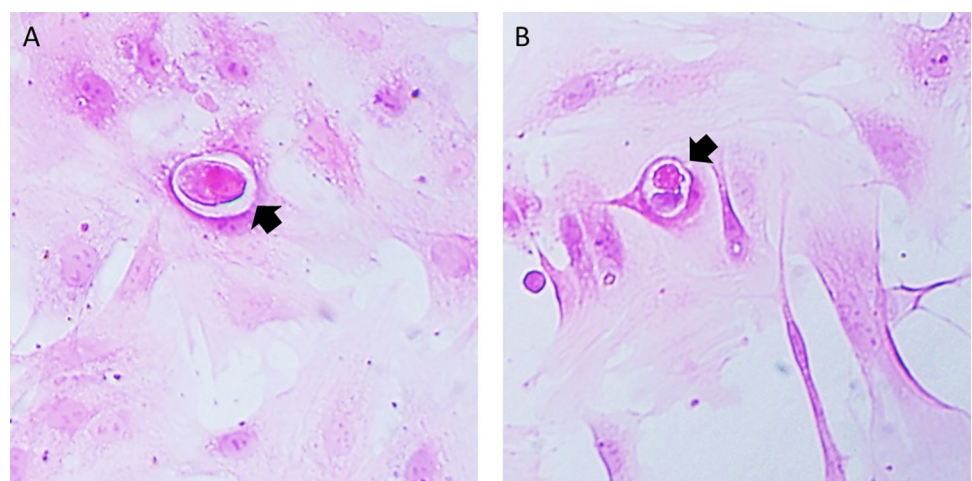


Fig 6. Intranuclear acidophilic IBs were observed at 24 h post-infection. (A) Fourth blind passage from horses, (B) fourth blind passage from goats. The black arrows indicate the intranuclear IB. Magnification: 200X. H&E staining.

<https://doi.org/10.1371/journal.pone.0290309.g006>

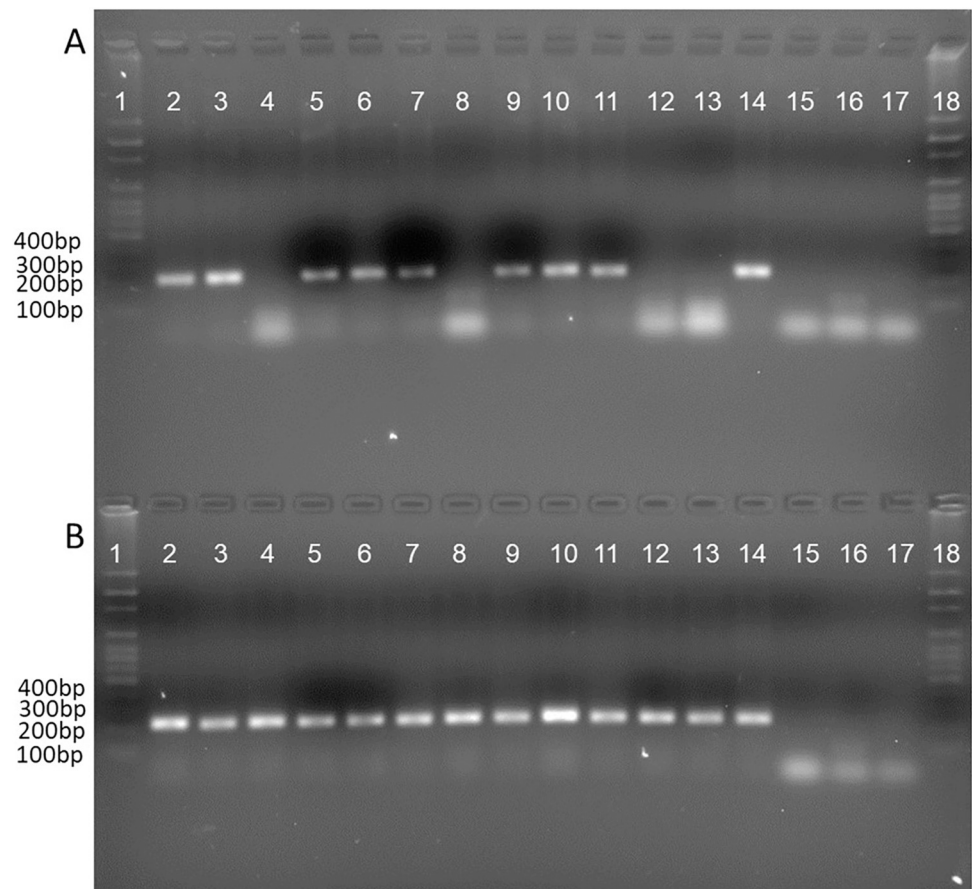


Fig 7. Agarose gel (1.5%) run in TAE 1X buffer. (A) Nested PCR of the first and second passages of primary cell cultures of rabbit testis. (1) Molecular weight marker 1 kb, (2) first blind passage from horses, (3) second blind passage from horses, (4) first blind passage from sheep, (5) second blind passage from sheep, (6) first blind passage from goats, (7) second blind passage from goats, (8) first blind passage from deer, (9) second blind passage from deer, (10) first blind passage from dairy cattle, (11) second blind passage from dairy cattle, (12) first blind passage from feedlot cattle, (13) second blind passage from feedlot cattle, (14) positive control, (15) negative control of amplification (NCA), (16) negative control of extraction (NCE), (17) non-inoculated primary cell cultures (NPCC), (18) molecular weight marker 1 kb. (B) Nested PCR of passages three and four in primary cell cultures of rabbit testis. (1) Marker of molecular weight of 100 bp, (2) third blind passage from horses, (3) fourth blind passage from horses, (4) third blind passage from sheep, (5) fourth blind passage from sheep, (6) third blind passage from goats, (7) fourth blind passage from goats, (8) third blind passage from deer, (9) fourth blind passage from deer, (10) third blind passage from dairy cattle, (11) fourth blind passage from dairy cattle, (12) third blind passage from feedlot cattle, (13) fourth blind passage from feedlot cattle, (14) positive control, (15) negative control of amplification (NCA), (16) negative control of extraction (CNE), (17) non-inoculated primary cell cultures (NPCC), (18) molecular weight marker 1 kb.

<https://doi.org/10.1371/journal.pone.0290309.g007>

from sheep and deer were positive until the second passage. However, the cell-free supernatant of feedlot cattle was negative by PCR until the third and fourth passages (Fig 7).

Viral replication kinetics

The growth kinetics study showed that the buffy coat lysate from horses replicated rapidly, and syncytia could be observed starting at 24 h post-infection in the 5th passage and up to 72 h in the 14th passage (Fig 8A).

The 4th and 5th passages achieved similar peak titers of $10^{4.1}$ TCID₅₀/mL and $10^{4.3}$ TCID₅₀/mL at 72 h post-infection, respectively. However, the 14th passage achieved higher peak titers of $10^{6.6}$ TCID₅₀/mL at 72 h post-infection. In addition, at 120 h post-infection, the viral titers decreased (Fig 8C).

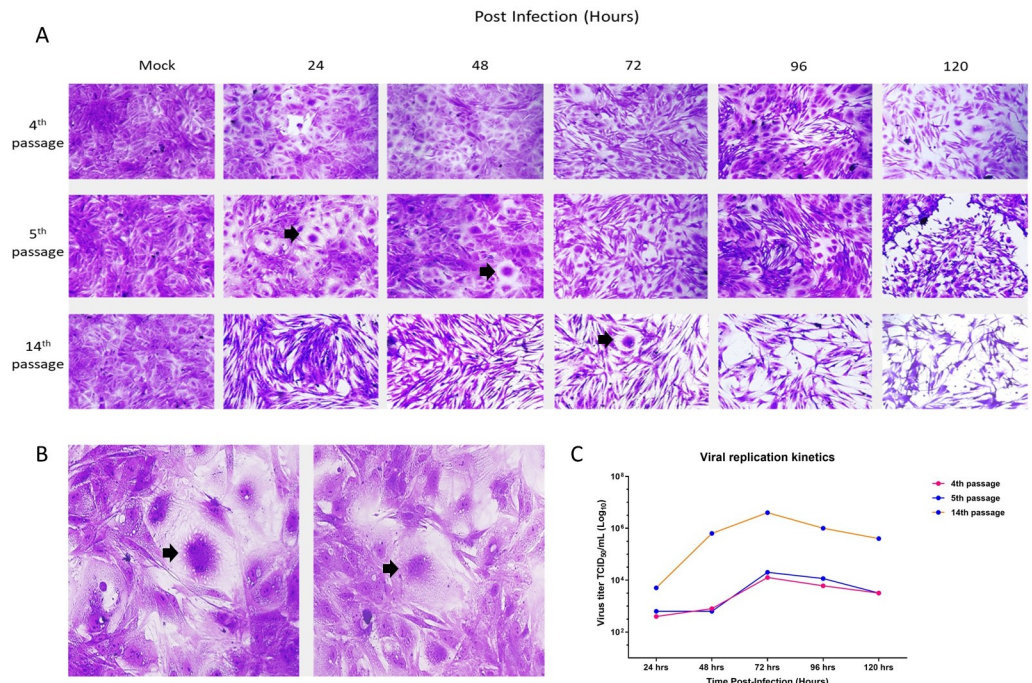


Fig 8. Growth kinetics of the cell-free supernatants from the 4th, 5th, and 14th passages of the buffy coat lysate from horses. (A) Cells inoculated with supernatant from the 4th passage, upper panel; supernatant from the 5th passage, middle panel; and supernatant from the 14th passage, lower panel. Magnification: 100X. (B) Syncytia were observed in the 5th passage at 24 h and 48 h post-infection (black arrows). Magnification: 200X. (C) Graph of viral titers at 24, 48, 72, 96, and 120 h post-infection corresponding to the 4th, 5th, and 14th passages of the buffy coat lysate from horses, where a maximum replication peak is observed at 72 h post-infection.

<https://doi.org/10.1371/journal.pone.0290309.g008>

Phylogenetic analysis

The alignment of the partial sequences of 422 bp of the *ORF75* gene indicated that the six partial sequences from the cell-free supernatants of the fourth passage from the different species affected by SA-MCF and the positive control of OvHV-2 shared 98%-99% nucleotide identity with other partial *ORF75* sequences obtained from the GenBank database. Regarding the structure of the inferred topology, the analysis indicated that our seven partial sequences present high homology with macariviruses with different OvHV-2 *ORF75* genes, reported in different parts of the world and separated from the clade of rhadinoviruses (human gammaherpesvirus 8) and from lymphocryptovirus (human gammaherpesvirus 4), found in different clades (Fig 9).

On the other hand, the *ORF75* partial sequences of the six cell-free supernatants of the fourth passage compared to the BJ1035 sequence, presented a non-synonymous substitution at position 1213, changing the amino acid (AA) from lysine (K) to threonine (T) (Table 3); however, the partial sequence of the sheep presented a second mutation at position 1314, changing the AA cysteine (C) to glycine (G) (Table 3), and therefore, they were classified as *ORF75**0201 due to the number of substitutions according to Russell's classification et al. (2014).

Immunocytochemistry (ICC) and immunofluorescence (IF) techniques

Positive cytoplasmic immunoreactivity to anti-OvHV-2 rabbit hyperimmune serum was observed in all wells inoculated with cell-free supernatants of the four blind passages from

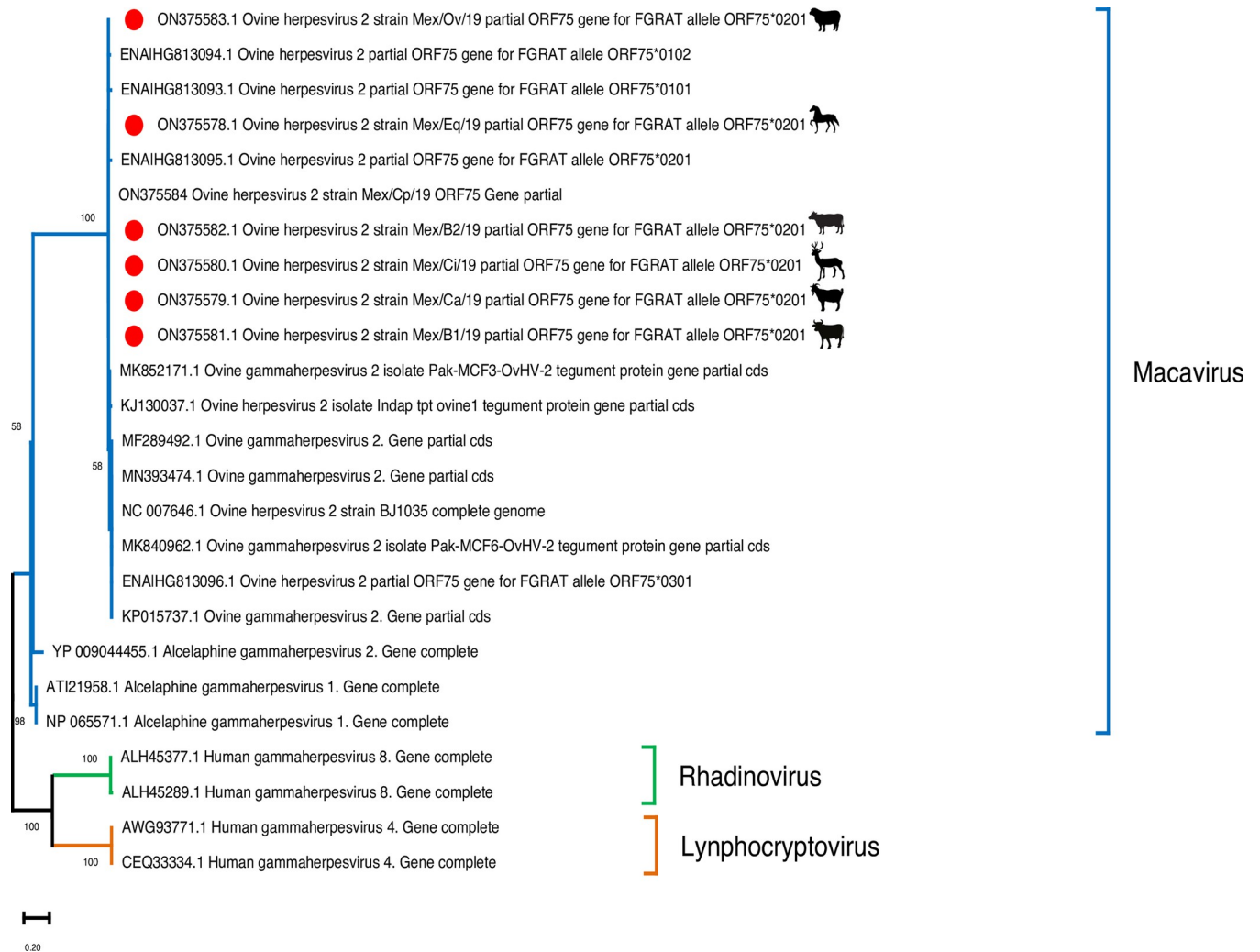


Fig 9. Phylogenetic analysis of partial sequences of the ORF75 gene. The tree is at scale, and the bar indicates the number of substitutions per site. The Mexican sequences are marked with red circles.

<https://doi.org/10.1371/journal.pone.0290309.g009>

Table 3. Genetic diversity of Mexican ORF75 sequences compared to the reference gene BJ1035.

GENE ORF75	NT [3637]	NT [3638]	NT [3639]	AA [1213]	NT [3940]	NT [3941]	NT [3942]	AA [1314]
*REF NC_007646.1 BJ1035	A	A	A	LYS	T	G	C	CYS
ON375578.1 (HORSE)	A	C	G	THR	-	-	-	NA
ON375579.1 (GOAT)	A	C	G	THR	-	-	-	NA
ON375580.1 (DEER)	A	C	G	THR	-	-	-	NA
ON375581.1 (DAIRY COW)	A	C	G	THR	-	-	-	NA
ON375582.1 (FEEDLOT CATTLE)	A	C	G	THR	-	-	-	NA
ON375583.1 (SHEEP)	A	C	G	THR	G	G	C	GLY

*Ref = reference, () = source, NT = nucleotides, AA = amino acids, [] = position, NA = does not apply.

<https://doi.org/10.1371/journal.pone.0290309.t003>

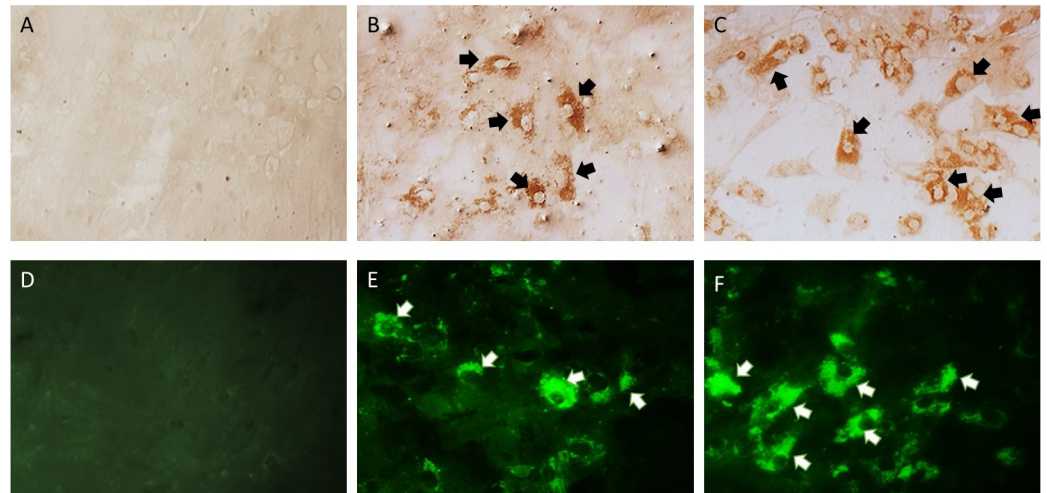


Fig 10. Cytoplasmic immunoreactivity with the ICC and IF techniques in primary cell cultures of rabbit testis cells. (A) ICC negative control, (B) ICC of the third passage from horses, (C) ICC of the third passage from goats, (D) IF negative control, (E) IF of the third passage from horses, (F) IF of the third passage from goats. Arrows indicate the cytoplasmic immunoreactivity appearing as an insoluble brown color for the ICC and a green-apple color for the IF. Magnification: 200X.

<https://doi.org/10.1371/journal.pone.0290309.g010>

horses, goats, dairy cattle, feedlot cattle, sheep, and deer. However, with the third blind passage of horses and goats, a higher proportion of cells (40% and 50% of the monolayer) with positive immunoreactivity to rabbit serum was observed (Fig 10). In contrast, wells inoculated with the third and fourth passages of feedlot cattle, dairy cattle, sheep, and deer had a lower proportion of cells (10% of the monolayer), with cytoplasmic immunoreactivity. Apple-green emission at 520 nm by IF and a brown precipitate by ICC were evident.

Deer liver immunohistochemistry

The cytoplasmic IBs of hepatocytes from the affected deer were immunoreactive to anti-OvHV-2 hyperimmune rabbit serum. In addition, also slight intranuclear immunoreactivity was also observed in hepatocytes (Fig 11).

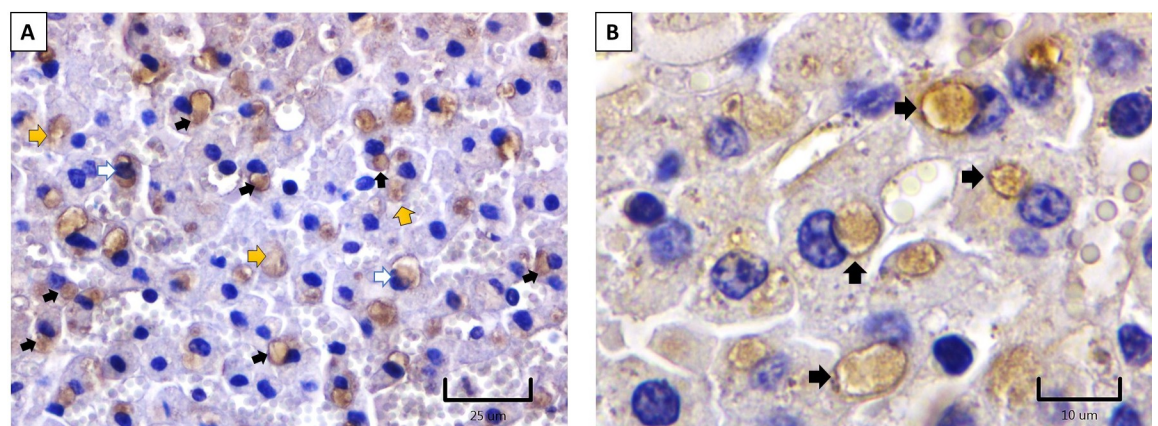


Fig 11. Deer liver immunohistochemistry. (A) and (B) Immunoreactivity to OvHV-2 antigens with rabbit hyperimmune serum in cytoplasmic IBs (black arrows), within the cytoplasm (yellow arrows), and in the nucleus of hepatocytes (white arrows).

<https://doi.org/10.1371/journal.pone.0290309.g011>

Discussion

An outbreak of SA-MCF that occurred in CEIEPAA, located in Tequisquiapan, state of Querétaro, Mexico, is described in the present study. The etiologic agent was identified and characterized as OvHV-2 using different diagnostic techniques, including IF, ICC, CPE, end-point PCR, and partial sequencing of the *ORF75* gene. During the outbreak, many animals of different species were affected, showing typical head-and-eye clinical signs compatible with SA-MCF and corneal opacity [11]. The microscopic lesions of vasculitis and perivasculitis in different organs and varying degrees of thrombosis and lymphoid hyperplasia in lymph nodes observed in deer that died during the SA-MCF outbreak are consistent with those reported by Brown et al. (1992) in white-tailed deer [42].

This study used buffy coats from affected animals to identify that they were infected with the OvHV-2 virus. This approach is similar to that of a study by Hristov et al. (2016), who used bison buffy coats, whole blood, lung, and spleen samples from differently affected animals during an outbreak of SA-MCF [26].

Primary cultures of rabbit testis were used for the *in vitro* identification of OvHV-2. The use of primary cultures to perform viral identification had already been reported previously for AIHV-1 and AIHV-2 [22, 24, 25]. From the third passage on primary cell cultures of rabbit testis, a marked CPE was observed at 72 h post-infection, consisting of small foci of refractile cytomegalic cells. This CPE was also described by Rossiter et al. (1980) during the identification and isolation of AIHV-1 [43].

In the present study, titers of the fourth blind passages from horses, goats, sheep, deer, feedlot cattle, and dairy cattle obtained in primary cell cultures of rabbit testis ranged from $\log 10^{2.8}$ to $\log 10^{4.19}$ TCID₅₀/mL. On the other hand, the cell-free supernatant from horses reached its highest peak of $10^{6.6}$ TCID₅₀/mL in passage 14 at 72 h post-infection. These results indicated that propagation of the OvHV-2 virus in primary rabbit testis cultures led to an increase in viral titers at each passage. This viral titer is similar to that found by Hristov et al. (2016) of 10^6 TCID₅₀/mL in Madin-Darby bovine kidney (MDBK) cells after passage 19 [26]. This increase in viral titers at higher passages could be because in the first passages, the virus is predominantly cell-associated, and after five passages, there is a period during which the viral genome undergoes rearrangements, leading to viral attenuation and resulting in better cell-free virus yields. However, this has only been shown in AIHV-1 [44]. In addition, in primary cultures of rabbit testis inoculated with buffy coats, we identified intranuclear acidophilic IB by H&E staining, which coincides with the results reported by Hristov et al. (2016) [26].

OvHV-2 was identified in primary cell cultures from rabbit testis through end-point nested PCR targeting a 238-bp fragment of the *ORF75* gene, with a greater intensity starting in the third and fourth passages in all cell-free supernatants from the different affected species. These results indicate that several blind passages are required to generate better cell-free virus yields and achieve adaptability of the virus to the cell, consistent with the report by Hristov et al. (2016) [26].

The buffy coat lysate from horses replicated with similar growth kinetics in the 4th and 5th passages, however, in the 14th passage, it reached a higher titer. Viral replication could be detected starting at 24 h post-infection due to syncyties formation only in the 5th passage and 14th passage. The CPE gradually increased, reaching a maximum at 72 h post-infection and the decrease in the viral titer at 120 h post-infection could be due to the death of cells. With these results, we can infer that primary cultures of rabbit testis support OvHV-2 replication. Our results agree with those of Hristov et al. (2016), in that the bison buffy coat was characterized by small syncytia at 24 h post-infection, and between 60–72 h post-infection there was more than 50% destruction of the monolayer [26].

Furthermore, the definitive diagnosis of OvHV-2 infection was confirmed using partial sequencing of the 422-bp fragment of the *ORF75* gene. Interestingly, the seven sequences from the cell-free supernatants of the fourth passage from different species affected by SA-MCF and the positive control of OvHV-2 shared 98%-99% nucleotide identity among them and with the OvHV-2 sequences reported in different regions of the world. These results align with those reported by Martins et al. (2017), who sequenced 13 positive samples of bovines from different areas of Brazil and found 97%-100% similarity with OvHV-2 from several other regions of the world [45].

In the present study, the *ORF75* sequences were classified as *ORF75*0201* for presenting at least one non-synonymous substitution, change from AA lysine to threonine; this indicates that the infectious agent that affected all animals during the 2018 outbreak with SA-MCF was the same strain as OvHV-2. On the other hand, our results differ from those of Russell et al. (2014) because they found that the major allele in 18 samples was *ORF75*0101*, which they found to be similar to the reference sequence BJ1035 [46, 47]. We can infer that in Mexico the most circulating allele is *ORF75*0201*. This could be a novel allele that allows infection between species that should be monitored. However, for genetic characterization and epidemiological studies, we would need to sequence the *ORF50* and *Ov9.5* genes, the latter being the most important for studies of this type [46]. In this sense, and with the results presented above, we could infer goats and sheep as sources of infection (transmission between species) or as potential reservoirs able to transmit to susceptible species (horses, deer, dairy cows, and feedlot cattle) due to their closeness to each other and sharing some of these grasslands.

The cytoplasmic immunoreactivity observed through IF and ICC in primary cell cultures from rabbit testis is equivalent to the intracytoplasmic immunoreactivity observed in multiple tissue samples affected by OvHV-2 using a monoclonal antibody (mAb-15A) targeted at a conserved epitope among all macaviruses [41]. In contrast, cytoplasmic acidophilic (eosinophilic) IBs immunoreactive to OvHV-2 using rabbit hyperimmune serum were observed in hepatocytes of deer that died during the SA-MCF outbreak. These results are consistent with those reported by Aluja et al. (1969), who described cytoplasmic acidophilic IBs in the neurons of cows infected with SA-MCF [29]. Similarly, our results are consistent with those reported by Goss et al. (1947), who described these IBs in Purkinje cells and epithelial cells of mucous membranes [48]. The cytoplasmic acidophilic IBs observed in the present study could be due to viral multiplication and the overproduction of viral and cellular proteins. These macromolecular aggregates, also called "dense bodies" in transmission electron microscopy, are very common in human cells inoculated with cytomegalovirus. Most of these structures are sequestered in Golgi-derived vesicles, and some dense bodies are located near or in contact with the nuclear envelope, where they appear to be transferred through nuclear pore viral proteins necessary for viral assembly [49]. The presence of acidophilic IB, as a manifestation of cytoplasmic accumulation of viral protein, also coincided with that described by Nelson et al. (2013), suggesting that cytoplasmic distribution of the capsid protein in OvHV-2 in infected terminal hosts represents abortive viral replication [9]. As a result, it can be speculated that cytoplasmic IBs in deer hepatocytes are formed by the accumulation of viral proteins necessary for virion assembly, in addition to abortive virions and cellular proteins. Further studies are needed to confirm this hypothesis.

Conclusions

The SA-MCF outbreak that affected CEIEPAA animals in Tequisquiapan, Queretaro, Mexico, was caused by the OvHV-2 virus. In addition, it was shown for the first time in Mexico that horses are susceptible to OvHV-2 infection and develop SA-MCF, so it should be considered

in the differential diagnosis of vesicular diseases in horses. Considering all results described above, we demonstrated that the buffy coats of CIEEPAA horses and *Artiodactyla* were infected with the OvHV-2 virus. Furthermore, we determined that primary rabbit testis cultures could be a good choice of cell culture model for OvHV-2 virus identification, as they support viral replication, CPE development, intranuclear IBs, and cytoplasmic immunoreactivity. However, to demonstrate the viral isolation of OvHV-2 in primary rabbit testis cultures, the disease needs to be reproduced in a susceptible host, through experimental inoculation with the isolate.

We also showed that the Mexican *ORF75* sequences shared 98%-99% nucleotide identity among them and with the OvHV-2 sequences reported in different regions of the world, and the *ORF75*0201* allele affected all animals in the CEIEPAA during the 2018 SA-MCF outbreak.

Supporting information

S1 Raw images.
(TIF)

Acknowledgments

Thanks to PAPIIT-UNAM (IN213321) and T.L. Madrigal-Valencia received a scholarship SEP-CONACYT, ID (968751). Thanks to the Special Cathedra “Dr. José E. Mota” 2019–2020. We would also like to thank the United States-Mexico Commission for the Prevention of Foot-and-Mouth Disease and Other Exotic Animal Diseases (CPA) for their technical support in laboratory testing and positive control. Special thanks to the histotechnologist Verónica Rodríguez Mata.

Author Contributions

Conceptualization: Tania Lucia Madrigal-Valencia, Jesús Hernández.

Formal analysis: Tania Lucia Madrigal-Valencia.

Investigation: Tania Lucia Madrigal-Valencia, Manuel Saavedra-Montañez, Humberto Ramírez-Mendoza.

Methodology: Tania Lucia Madrigal-Valencia, Manuel Saavedra-Montañez, Armando Pérez-Torres, Jesús Hernández, Joaquim Segalés, Yesmín Domínguez Hernández, Irma Eugenia Candanosa-Aranda, Alfredo Pérez-Guiot.

Resources: Yesmín Domínguez Hernández, Irma Eugenia Candanosa-Aranda, Alfredo Pérez-Guiot.

Supervision: Manuel Saavedra-Montañez, Armando Pérez-Torres, Jesús Hernández, Joaquim Segalés.

Writing – original draft: Tania Lucia Madrigal-Valencia.

Writing – review & editing: Tania Lucia Madrigal-Valencia, Manuel Saavedra-Montañez, Armando Pérez-Torres, Jesús Hernández, Joaquim Segalés.

References

1. O’toole D, Li H. The Pathology of malignant catarrhal fever, with an emphasis on ovine herpesvirus 2. *Vet Pathol* 2014; 51:437–52. <https://doi.org/10.1177/0300985813520435> PMID: 24503439

2. Russell GC, Stewart JP, Haig DM. Malignant catarrhal fever: a review. *Vet J* 2009; 179:324–35. <https://doi.org/10.1016/j.tvjl.2007.11.007> PMID: 18760944
3. Amoroso MG, Galiero G, Fusco G. Genetic characterization of ovine herpesvirus 2 strains involved in water buffaloes malignant catarrhal fever outbreaks in Southern Italy. *Vet Microbiol* 2017; 199:31–5. <https://doi.org/10.1016/j.vetmic.2016.12.020> PMID: 28110782
4. Li H, Brooking A, Cunha CW, Highland MA, O'Toole D, Knowles DP, et al. Experimental induction of malignant catarrhal fever in pigs with ovine herpesvirus 2 by intranasal nebulization. *Vet Microbiol* 2012; 159:485–9. <https://doi.org/10.1016/j.vetmic.2012.04.016> PMID: 22560763
5. Foyle KL, Fuller HE, Higgins RJ, Russell GC, Willoughby K, Rosie WG, et al. Malignant catarrhal fever in sika deer (*Cervus nippon*) in the UK. *Vet Rec* 2009; 165:445–7. <https://doi.org/10.1136/vr.165.15.445> PMID: 19820260
6. Costa ÉA, Bomfim MRQ, Da Fonseca FG, Drumond BP, Coelho FM, Vasconcelos AC, et al. Ovine herpesvirus 2 infection in Foal, Brazil. *Emerg Infect Dis* 2009; 15:844–5. <https://doi.org/10.3201/eid1505.081664> PMID: 19402994
7. Gailbreath KL, Taus NS, Cunha CW, Knowles DP, Li H. Experimental infection of rabbits with ovine herpesvirus 2 from sheep nasal secretions. *Vet Microbiol* 2008; 132:65–73. <https://doi.org/10.1016/j.vetmic.2008.04.035> PMID: 18539411
8. Li H, Cunha CW, Taus NS. Malignant catarrhal fever: understanding molecular diagnostics in context of epidemiology. *Int J Mol Sci* 2011; 12:6881–93. <https://doi.org/10.3390/ijms12106881> PMID: 22072925
9. Nelson DD, Taus NS, Schneider DA, Cunha CW, Davis WC, Brown WC, et al. Fibroblasts express OvHV-2 capsid protein in vasculitis lesions of American bison (*Bison bison*) with experimental sheep-associated malignant catarrhal fever. *Vet Microbiol* 2013; 166:486–92. <https://doi.org/10.1016/j.vetmic.2013.07.021> PMID: 23953727
10. Sood R, Kumar N, Bhatia S. Malignant catarrhal fever. *Emerging and re-emerging infectious diseases of livestock* 2017:347–62. https://doi.org/10.1007/978-3-319-47426-7_16/TABLES/2.
11. O'Toole D, Li H, Sourk C, Montgomery DL, Crawford TB. Malignant catarrhal fever in a bison (*Bison bison*) feedlot, 1993–2000. *J Vet Diagn Invest* 2002; 14:183–93. <https://doi.org/10.1177/104063870201400301> PMID: 12033673
12. Traul DL, Taus NS, Oaks JL, O'Toole D, Rurangirwa FR, Baszler T V., et al. Validation of nonnested and real-time PCR for diagnosis of sheep-associated malignant catarrhal fever in clinical samples. *J Vet Diagn Invest* 2007; 19:405–8. <https://doi.org/10.1177/104063870701900412> PMID: 17609352
13. Wan SK, Castro AE, Heuschele WP, Ramsay EC. Enzyme-linked immunosorbent assay for the detection of antibodies to the alcelaphine herpesvirus of malignant catarrhal fever in exotic ruminants. *Am J Vet Res* 1988; 49:164–8. PMID: 3348526
14. Rossiter PB. Immunofluorescence and immunoperoxidase techniques for detecting antibodies to malignant catarrhal fever in infected cattle. *Trop Anim Health Prod* 1981; 13:189–92. <https://doi.org/10.1007/BF02237922> PMID: 7046177
15. Herring A, Reid H, Inglis N, Pow I. Immunoblotting analysis of the reaction of wildebeest, sheep and cattle sera with the structural antigens of alcelaphine herpesvirus-1 (malignant catarrhal fever virus). *Vet Microbiol* 1989; 19:205–15. [https://doi.org/10.1016/0378-1135\(89\)90067-9](https://doi.org/10.1016/0378-1135(89)90067-9).
16. Sentsui H, Nishimori T, Nagai I, Nishioka N. Detection of sheep-associated malignant catarrhal fever virus antibodies by complement fixation tests. *J Vet Med Sci* 1996; 58:1–5. <https://doi.org/10.1292/jvms.58.1> PMID: 8645750
17. Li H, Shen DT, Knowles DP, Gorham JR, Crawford TB. Competitive inhibition enzyme-linked immunosorbent assay for antibody in sheep and other ruminants to a conserved epitope of malignant catarrhal fever virus. *J Clin Microbiol* 1994; 32:1674–9. <https://doi.org/10.1128/jcm.32.7.1674-1679.1994> PMID: 7523438
18. Mushi EZ, Plowright W. A microtitre technique for the assay of malignant catarrhal fever virus and neutralizing antibody. *Res Vet Sci* 1979; 27:230–2. [https://doi.org/10.1016/S0034-5288\(18\)32835-2](https://doi.org/10.1016/S0034-5288(18)32835-2).
19. Decaro N, Tinelli A, Pratelli A, Martella V, Tempesta M, Buonavoglia C. First two confirmed cases of malignant catarrhal fever in Italy. *New Microbiol* 2003; 26:339–44. PMID: 14596344
20. Dubuisson J, Thiry E, Bublot M, Sneyers M, Boulanger D, Guillaume J, et al. Production and characterization of monoclonal antibodies to bovid herpesvirus-4. *Vet Microbiol* 1989; 19:305–15. [https://doi.org/10.1016/0378-1135\(89\)90096-5](https://doi.org/10.1016/0378-1135(89)90096-5) PMID: 2546320
21. Li H, Shen DT, O'Toole D, Knowles DP, Gorham JR, Crawford TB. Investigation of sheep-associated malignant catarrhal fever virus infection in ruminants by PCR and competitive inhibition enzyme-linked immunosorbent assay. *J Clin Microbiol* 1995; 33:2048–53. <https://doi.org/10.1128/jcm.33.8.2048-2053.1995> PMID: 7559946

22. Plowright W, Ferris RD, Scott GR. Blue wildebeest and the aetiological agent of bovine malignant catarrhal fever. *Nature* 1960; 188:1167–9. <https://doi.org/10.1038/1881167a0> PMID: 13736396
23. Alhajri SM, Cunha CW, Knowles DP, Li H, Taus NS. Evaluation of glycoprotein Ov8 as a potential antigen for an OvHV-2-specific diagnostic assay. *PLoS One* 2018; 13:e0200130. <https://doi.org/10.1371/journal.pone.0200130> PMID: 29966004
24. Plowright W, Ferris RD. The preparation of bovine thyroid monolayers for use in virological investigations. *Res Vet Sci* 1961; 2:149–53. [https://doi.org/10.1016/S0034-5288\(18\)34967-1](https://doi.org/10.1016/S0034-5288(18)34967-1).
25. Castro AE, Daley GG, Zimmer MA, Whitenack DL, Jensen J. Malignant catarrhal fever in an Indian gaur and greater kudu: experimental transmission, isolation, and identification of a herpesvirus. *Am J Vet Res* 1982; 43:5–11. PMID: 7091816
26. Hristov M V, Peshev RD. Isolation, and identification of malignant catarrhal fever virus in cell cultures. *Bulg J Vet Med* 2016; 19:263–73. <https://doi.org/10.15547/BJVM.935>.
27. Li H, Taus NS, Jones C, Murphy B, Evermann JF, Crawford TB. A devastating outbreak of malignant catarrhal fever in a bison feedlot. *J Vet Diagn Invest* 2006; 18:119–23. <https://doi.org/10.1177/104063870601800120> PMID: 16566270
28. Headley SA, de Oliveira TES, Cunha CW. A review of the epidemiological, clinical, and pathological aspects of malignant catarrhal fever in Brazil. *Braz J Microbiol* 2020; 51:1405–32. <https://doi.org/10.1007/s42770-020-00273-6> PMID: 32542424
29. Aluja A, Rocha TC De, Velázquez A. Fiebre catarral maligna. *Rev Mex Cienc Pecu* 1969:1–8. <https://doi.org/10.22319/RMCP.V0112>.
30. Pérez-Guiot A, Páez-Trejo A, Domínguez-Hernández Y, Carranza-Velázquez J, Hernández-García D, Carrisoza-Urbina I, et al. Malignant catarrhal fever associated with ovine gammaherpesvirus-2 in domestic ruminants in Queretaro, Mexico. *Pak Vet J* 2022; 43:61–6. <https://doi.org/10.29261/pakvetj/2022.076>.
31. English D, Andersen BR. Single-step separation of red blood cells. Granulocytes and mononuclear leukocytes on discontinuous density gradients of Ficoll-Hypaque. *J Immunol Methods* 1974; 5:249–52. [https://doi.org/10.1016/0022-1759\(74\)90109-4](https://doi.org/10.1016/0022-1759(74)90109-4) PMID: 4427075
32. Baxter SIF, Pow I, Bridgen A, Reid HW. PCR detection of the sheep-associated agent of malignant catarrhal fever. *Arch Virol* 1993; 132:145–59. <https://doi.org/10.1007/BF01309849> PMID: 8352654
33. Roche. High Pure PCR Template Preparation Kit 2020;27.
34. Reed LJ, Muench H. A simple method of estimating fifty percent endpoints. *Am J Epidemiol* 1938; 27:493–7. <https://doi.org/10.1093/OXFORDJOURNALS.AJE.A118408/2/27-3-493.PDF.GIF>.
35. Hall TA. BioEdit a user-friendly biological sequence alignment editor and analysis program for Windows 95/98/NT. *Scientific Research Publishing* 1999:95–8. [https://www.scirp.org/\(S\(lz5mqp453edsnp55rrjct55\)\)/reference/ReferencesPapers.aspx?ReferenceID=1383440](https://www.scirp.org/(S(lz5mqp453edsnp55rrjct55))/reference/ReferencesPapers.aspx?ReferenceID=1383440) (accessed July 10, 2023).
36. Tamura K, Stecher G, Kumar S. MEGA11: molecular evolutionary genetics analysis version 11. *Mol Biol Evol* 2021; 38:3022–7. <https://doi.org/10.1093/molbev/msab120> PMID: 33892491
37. Johnson M, Zaretskaya I, Raytselis Y, Merezhuik Y, McGinnis S, Madden TL. NCBI BLAST: a better web interface. *Nucleic Acids Res* 2008;36. <https://doi.org/10.1093/NAR/GKN201>.
38. Posada D. jModelTest: phylogenetic model averaging. *Mol Biol Evol* 2008; 25:1253–6. <https://doi.org/10.1093/molbev/msn083> PMID: 18397919
39. Tamura K, Nei M. Estimation of the number of nucleotide substitutions in the control region of mitochondrial DNA in humans and chimpanzees. *Mol Biol Evol* 1993; 10:512–26. <https://doi.org/10.1093/oxfordjournals.molbev.a040023> PMID: 8336541
40. Orós J, Poveda JB, Rodríguez JL, Franklin CL, Fernández A. Natural cilia-associated respiratory bacillus infection in rabbits used for elaboration of hyperimmune serum against *Mycoplasma* sp. *Zentralbl Veterinarmed B* 1997; 44:313–7. <https://doi.org/10.1111/j.1439-0450.1997.tb00980.x> PMID: 9270356
41. Headley SA, de Lemos GAA, Dall Agnol AM, Xavier AAC, Depes VCA, Yasumitsu CY, et al. Ovine gammaherpesvirus 2 infections in cattle without typical manifestations of sheep-associated malignant catarrhal fever and concomitantly infected with bovine coronavirus. *Braz J Microbiol* 2022; 53:433–46. <https://doi.org/10.1007/s42770-021-00653-6> PMID: 34780031
42. Brown CC, Bloss LL. An epizootic of malignant catarrhal fever in a large captive herd of white-tailed deer (*Odocoileus virginianus*). *J Wildl Dis* 1992; 28:301–5. <https://doi.org/10.7589/0090-3558-28.2.301>.
43. Rossiter PB. A lack of readily demonstrable virus antigens in the tissues of rabbits and cattle infected with malignant catarrhal fever virus. *Br Vet J* 1980; 136:478–83. [https://doi.org/10.1016/s0007-1935\(17\)32190-5](https://doi.org/10.1016/s0007-1935(17)32190-5) PMID: 6784880

44. Wright H, Stewart JP, Ileri RG, Campbell I, Pow I, Reid HW, et al. Genome re-arrangements associated with loss of pathogenicity of the γ -herpesvirus alcelaphine herpesvirus-1. *Res Vet Sci* 2003; 75:163–8. [https://doi.org/10.1016/S0034-5288\(03\)00043-2](https://doi.org/10.1016/S0034-5288(03)00043-2).
45. Martins M de SN, Castro AMMG de, Lima M dos S, Pinto V da SC, Silva TG da, Fava C Del, et al. Malignant Catarrhal Fever in Brazilian cattle presenting with neurological syndrome. *Braz J Microbiol* 2017; 48:366–72. <https://doi.org/10.1016/j.bjm.2016.10.021> PMID: 28081979
46. Russell GC, Scholes SF, Twomey DF, Courtenay AE, Grant DM, Lamond B, et al. Analysis of the genetic diversity of ovine herpesvirus 2 in samples from livestock with malignant catarrhal fever. *Vet Microbiol* 2014; 172:63–71. <https://doi.org/10.1016/j.vetmic.2014.04.011> PMID: 24846753
47. Hart J, Ackermann M, Jayawardane G, Russell G, Haig DM, Reid H, et al. Complete sequence and analysis of the ovine herpesvirus 2 genome. *J Gen Virol* 2007; 88:28–39. <https://doi.org/10.1099/vir.0.82284-0> PMID: 17170433
48. Goss LW, Cole CR, Kissling RE. The pathology of malignant catarrhal fever (Bovine epitheliosis): with special reference to cytoplasmic inclusions. *Am J Pathol* 1947; 23:837. PMID: 19970964
49. Severi B, Landini MP, Cenacchi G, Zini N, Maraldi NM. Human cytomegalovirus nuclear and cytoplasmic dense bodies. *Arch Virol* 1992; 123:193–207. <https://doi.org/10.1007/BF01317149> PMID: 1372496